Neutrino Propagation in the Sun: A Study of the MSW Effect

Author: Marta Giral López, mgirallo10@alumnes.ub.edu
Facultat de Física, Universitat de Barcelona, Diagonal 645, 08028 Barcelona, Spain.

Advisor: Jordi Salvadó, jsalvado@ub.edu

Abstract: The discovery of neutrino oscillations solved the solar neutrino problem but contradicts the Standard Model by having non-zero mass neutrinos, hinting at new physics beyond the SM. In this work, the impact of the Mikheyev-Smirnov-Wolfenstein (MSW) or matter effect in two-neutrino oscillations is studied via numerical simulation and results are compared with the adiabatic approximation (the analytical approach) and latest experimental data from neutrino detectors. The numerical resolution also allows to incorporate Non-Standard Interactions parametrized by a scalar ε, weighted in respect to the matter potential. Results show that numerical values are in agreement with the adiabatic approximation and the Standard and Non-Standard Interactions for the studied range of ε, not constrained by experimental data.
Keywords: Solar neutrinos, neutrino oscillations, MSW effect, Non-Standard Interactions
SDGs: Quality Education; Industry, Innovation and Infrastructure; Reduced Inequalities.

I. INTRODUCTION

The Sun is our principal source of neutrinos, produced via thermonuclear reactions in its core, which is mostly made of hydrogen (around 74%), helium (around 24%) and less than 2% of heavier elements. The extreme conditions of temperature and density at the core make nuclear reactions that convert hydrogen into helium possible, through the proton-proton (pp) chain and the carbon-nitrogen-oxygen (CNO) cycle. In the Sun, a relatively low mass star, 99% of the total energy production is due to the pp chain [1].

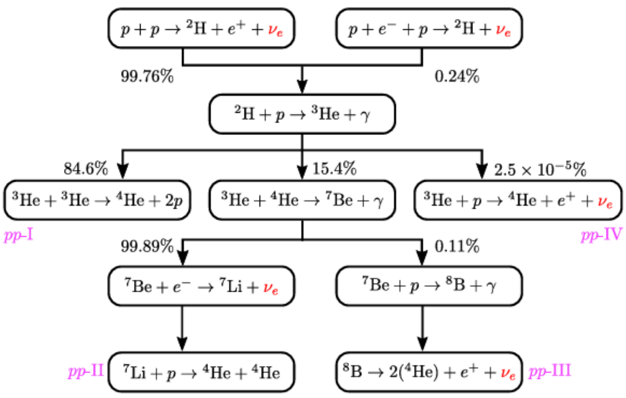

Figure 1: Nuclear reactions in the pp chain. Produced neutrinos are highlighted. Source: [1].

Fig. 1 shows the five different reactions that can be identified as sources of electronic neutrinos, referred to as pp, pep, hep, ^{7}Be and ^{8}B neutrinos. As the initial particles are all non-relativistic, neutrinos from nuclear reactions that have two final particles are monochromatic (pep and ^{7}Be), as their kinetic energy is fixed. In contrast, reactions with three final particles give neutrinos with a spectra of energies (pp, hep, ^{8}B), as shown in Fig. 2. The two monochromatic lines of the ^{7}Be neutrinos correspond to the two possible outcomes of the reaction ${}^7\mathrm{Be} + e^- \to {}^7\mathrm{Li} + \nu_e$, which can give lithium in its excited state or ground state [1].

This production of solar neutrinos is predicted by the Solar Standard Model (SSM), a mathematical model of the Sun as a spherical ball of gas constrained by well-determined quantities such as its mass, radius and luminosity. Knowing the rates of the thermonuclear reactions at the core, Bahcall et al. [2] computed the theoretical neutrino flux at the Earth.

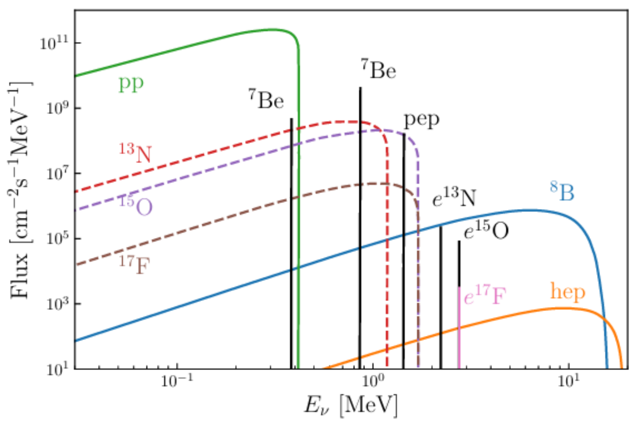

Figure 2: Theoretical neutrino fluxes predicted by the Solar Standard Model (SSM) and their corresponding energy spectra for neutrinos produced by the pp chain and the CNO cycle. Source: [1].

The first solar neutrino detection was the Homestake experiment by Raymond Davis in the late 1960s, in which the solar neutrino experimental flux differed greatly from Bahcall's prediction, being around one third of the expected value [3]. This was named the *solar neutrino problem*, solved years later by neutrino oscillations that implied that neutrinos have mass, as opposed to the Standard Model theory, hinting at physics beyond this model. Furthermore, neutrino oscillations are affected by the matter potential when not in vacuum, known as the MSW effect, discovered by Mikheyev, Smirnov and Wolfenstein [4], [5].

The aim of this work is to study neutrino propagation in the Sun under the MSW effect, introducing Non-Standard physics and observing its compatibility with the experimental data [6]. Evolution of neutrino states from production point to their arrival to Earth detectors is computed numerically in a simulation and is also compared with the results obtained using the adiabatic approximation [1], [7], and a LMA-MSW (Large Mixing Angle) numerical approach [8].

II. THEORETICAL BACKGROUND

Neutrino oscillations is a quantum mechanical phenomenon that occurs due to non-zero neutrino masses. This effect arises from the mixing between their mass eigenstate ν_i $(i = 1, 2, 3)$ and their flavor eigenstate ν_α $(\alpha = e, \mu, \tau)$, which is a superposition of mass states. When propagating through space, each mass state has a different phase due to the difference in masses, resulting in a different superposition of mass eigenstates and corresponding flavor eigenstate. This quantum state propagates coherently and periodically, leading to periodic oscillations when in vacuum [1].

The two sets of eigenstates are related by a unitary transformation,

$$\begin{aligned} |\nu_\alpha\rangle &= \sum_i U_{\alpha i} |\nu_i\rangle , \\ |\nu_i\rangle &= \sum_\alpha U^*_{\alpha i} |\nu_\alpha\rangle , \end{aligned} \tag{1}$$

where $U_{\alpha i}$ is the Pontecorvo–Maki–Nakagawa–Sakata matrix (PMNS or lepton mixing matrix) [1].

The evolution of the flavor eigenstates is determined by the Schrödinger equation. In matrix notation for the three-flavor neutrino oscillations in vacuum and using natural units ($c = \hbar = 1$),

$$i\frac{d}{dL}\begin{pmatrix} \nu_e \\ \nu_\mu \\ \nu_\tau \end{pmatrix} = \frac{1}{2E_\nu} U \begin{pmatrix} m_1^2 & 0 & 0 \\ 0 & m_2^2 & 0 \\ 0 & 0 & m_3^2 \end{pmatrix} U^\dagger \begin{pmatrix} \nu_e \\ \nu_\mu \\ \nu_\tau \end{pmatrix}, \tag{2}$$

with L the propagation distance, E_ν the neutrino energy and m_i the masses of ν_i.

In the Sun, only two neutrinos participate significantly in the mixing, the electron neutrino and either the muon neutrino or a superposition of muon and tau neutrinos. Matter effects need to be considered: neutrinos interact with matter via weak interaction, and its only significant contribution comes from coherent forward scattering of electron neutrinos with medium particles [1]. Consequently, an effective potential V_e that accounts for the MSW matter effect needs to be introduced to the Hamiltonian. With these two changes, we obtain the following Hamiltonian in the two-flavor neutrino framework,

$$\mathcal{H} = \frac{1}{2E_\nu} U \begin{pmatrix} m_1^2 & 0 \\ 0 & m_2^2 \end{pmatrix} U^\dagger + \begin{pmatrix} V_e(L) & 0 \\ 0 & 0 \end{pmatrix}, \tag{3}$$

and now the mixing matrix is [7]

$$U = \begin{pmatrix} \cos\theta & \sin\theta \\ -\sin\theta & \cos\theta \end{pmatrix}, \tag{4}$$

where θ is the mixing angle, which quantifies the entanglement of the neutrino states in vacuum. The latest value of this angle for the electron and muon mixing is $\theta = 33.76^{+0.42}_{-0.41}{}^\circ$ [6].

Neutrino detection measures the survival probabilities of each flavor, for example the electron neutrino survival probability at a given propagation distance L is computed as $P(\nu_e \to \nu_e) = |\langle \nu_e(L)|\nu_e(0)\rangle|^2$. As anything proportional to the identity in the Hamiltonian will only induce a global phase leaving the probability unchanged, it is possible to further modify it by subtracting $m_1^2/2E_\nu \mathbb{I}$. After operating with U, $U^\dagger$, the final Hamiltonian is

$$\mathcal{H} = \frac{\Delta m^2}{4E_\nu} \begin{pmatrix} -\cos2\theta + \frac{4E_\nu}{\Delta m^2} V_e & \sin2\theta \\ \sin2\theta & \cos2\theta \end{pmatrix}, \tag{5}$$

where $\Delta m^2 \equiv m_2^2 - m_1^2 = 7.537^{+0.094}_{-0.10} \cdot 10^{-5}$ eV^2 [6]. The effective potential is $V_e = \sqrt{2} G_F N_e$ [4], where G_F is the Fermi constant and N_e the electron density in the Sun, which depends on L, the distance to the center. The electron density according to the Standard Solar Model (BP2000) can be accurately modeled by an exponential, $N_e(L) = N_e(0)\exp(-10.54L/R_\odot)$, where $N_e(0) = 245N_A$ is the electron density at the neutrino production point and N_A the Avogadro number [2].

Additionally, interactions that deviate from the Standard Model (Non-Standard Interactions, NSI) can be considered by introducing extra potential terms on the Hamiltonian parametrized by ε, which can be on the diagonal or off-diagonal in flavor [9]:

$$\begin{pmatrix} V_e & 0 \\ 0 & 0 \end{pmatrix} + V_e \begin{pmatrix} \varepsilon_1 & \varepsilon_{nd} \\ \varepsilon_{nd} & \varepsilon_2 \end{pmatrix} = \begin{pmatrix} V_e(1-\varepsilon') & \varepsilon_{nd} \\ \varepsilon_{nd} & 0 \end{pmatrix}, \tag{6}$$

Contributions from the diagonal (ε') and non-diagonal (ε_{nd}) terms will be studied separately.

III. RESULTS AND DISCUSSION

In order to solve the differential equation (Eq. A1 in Appendix A) and obtain the temporal evolution of flavor states, one can either solve analytically by applying the adiabatic approximation (for high energies only) or compute the solution numerically. The latter allows for an exact solution at any given energy, not bounded by the validity limits of the approximation. This approximation takes advantage of the matter potential variation being much slower than the oscillations, and thus the neutrino quantum state is always an eigenstate of the Hamiltonian and transitions smoothly from a flavor eigenstate to a mass eigenstate. According to this, the survival probability in function of the energy is

$$P_{ee}(E) \approx \frac{1}{2}[1 + \cos 2\theta_m \cos 2\theta], \tag{7}$$

where θ_m is the effective mixing angle (that is, making $\mathcal{H}$ diagonal in terms of an effective mass difference Δm_m^2 and the effective mixing angle). For low energies, this probability is $P_{ee} \approx 0.57$ and for high energies is $P_{ee} \approx 0.3$ [1].

The numerical simulation uses the iterative method Runge-Kutta of 4th order (RK4) to obtain the evolved states at many given lengths $|\nu_e(L)\rangle$, $|\nu_\mu(L)\rangle$, and the instantaneous survival probability for both flavors is computed as it advances with a variable potential $V_e(L)$. Fixing the energy, it is possible to observe the oscillations in probability as a function of the length traveled inside the Sun. Furthermore, the average wavelength is determined by identifying maximums in probability and obtaining the distance between them. This parameter serves as an indicator of how fast compared to the radius of the Sun—and hence the potential evolution inside it—are the oscillations. Once the state is propagated to $L = R_\odot$, neutrinos are outside the Sun and perform vacuum oscillations ($V_e \to 0$ for $L \to R_\odot$), meaning the differential equation A1 is now solvable analytically and a simple propagation function is required in order to minimize computational power needed. In the mass base the Hamiltonian is diagonal, implying that the evolution of mass eigenstates is

$$|\nu_i(L)\rangle = e^{-i\frac{\Delta m^2}{2E_\nu}L} |\nu_i(0)\rangle . \tag{8}$$

The survival probability as a function of L and the energy of the produced electron neutrino E_ν is

$$P_{e\to e}(L) = 1 - \sin^2(2\theta)\sin^2\left(\frac{\Delta m^2 L}{4E_\nu}\right). \tag{9}$$

Therefore, the flavor eigenstate that left the Sun undergoes a basis transformation and propagates to the Earth according to Eq. 8. Then, the transformation is reversed to obtain again the state in flavor basis and compute the final survival probability of an electron neutrino created at the center of the Sun after propagating to the Earth and being detected. This final probability is evaluated by evolving in vacuum the final state of the propagation in the Sun a number of oscillation periods large enough so the statistical study can be performed, and averaging the probability in this interval ΔL, as vacuum oscillations are extremely fast and the detectors' resolution is not sufficiently high to account for them. Taking advantage of the fact that the vacuum propagation equation can be solved easily (Hamiltonian is diagonal in the mass basis), this evolution is performed analytically rather than numerically with RK4. The probability average is computed by numerically integrating the probability with a Monte Carlo method between $R_\odot$ and $R_\odot + \Delta L$ and dividing by this same ΔL. Numerical parameters of this integral have been set so that the associated error is four orders of magnitude smaller or less.

Neutrino energy spectra ranges typically from 0.1 to 20 MeV, as shown in Fig. 2. Taking a look at the form of the Hamiltonian (Eq. 3), one can infer the nature of the state at the limits of low and high energies:

- At low energies, the mass term dominates over the matter potential and the MSW effect is negligible, being almost identical to vacuum propagation. The created neutrino at the center of the Sun is of electronic flavor, and when propagating it will have maximal oscillations, as if it were propagating in vacuum.

- At high energies, the opposite effect happens and the relevant contribution to the Hamiltonian is now the matter potential V_e. Consequently, the neutrino flavor state is an eigenstate of the Hamiltonian and barely oscillates. However, these oscillations are much faster than the propagation: the wavelength of the oscillation is many orders of magnitude smaller than the radius of the Sun. As the neutrino propagates through the Sun, the matter potential decreases exponentially but adiabatically, i.e. much slowly compared to neutrino oscillations, making it a soft transition. As a result, the neutrino state is always an eigenstate although it is no longer in flavor basis as the Hamiltonian changes with L, and in the end the state going out of the Sun is a mass eigenstate. When this mass eigenstate propagates through vacuum to Earth, the evolution phase is a global phase and probability is constant.

After all these steps for a single value of the neutrino energy, a loop is done to cover the whole neutrino energy spectrum. The only difference between the procedure for NSI compared to the Standard Interactions is the addition of ε parameters to the Hamiltonian that measure the relative strength of the interaction compared to the matter potential.

A. Standard Interactions (SI)

To test the code, matter potential can be set to zero (vacuum oscillations) and compare the obtained results with the analytical expression for the probability, Eq. 9.

The numerical results follow closely the theoretical values, as shown in Appendix B. In the two-neutrino framework, the sum of both probabilities is logically 1. The amplitude of the oscillation is not 1 due to the mixing angle, the term $\sin^2(2\theta)$, meaning that a neutrino that has been created with electron flavor can never become a muon neutrino by propagating and vice versa.

Afterwards, the matter potential $V_e(L) = \sqrt{2}G_F N_e(L)$ is introduced, which depends on the distance traversed from the center of the Sun. For different energies, the following evolutions are obtained:

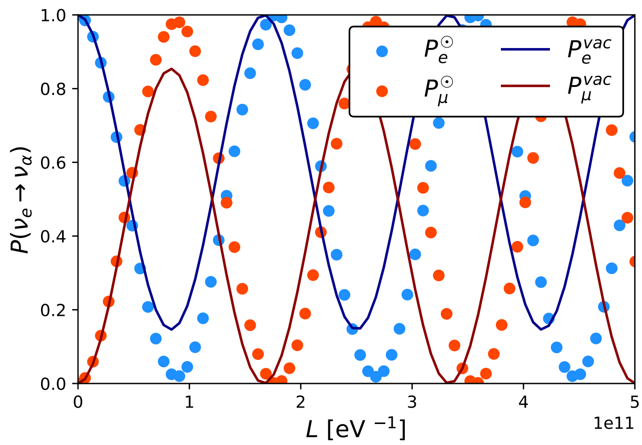

Figure 3: Probability of an electron neutrino changing its flavor (P_μ) or not (P_e) in function of traversed distance L, for a fixed energy $E_\nu = 1$ MeV. $P^{\rm vac}$ are the theoretical values of the probability in vacuum (Eq. 8) and $P^{\odot}$ the numerical values of the probability in the Sun considering the matter potential V_e.

In Fig. 3, evolution for neutrino energy $E_\nu = 1$ MeV (relatively low energy) in the inner part of the Sun ($R_\odot \approx 3.5 \cdot 10^{15}$ eV^{-1}) is similar to vacuum oscillations and starts deviating from that behavior with distance due to the MSW effect. Oscillation wavelength affected by the potential is larger than vacuum wavelength, as expected. As mentioned before, in this low energy limit the oscillation is maximal as the matter potential is almost negligible and does not undergo significant changes throughout the whole propagation in the Sun. The amplitude is now near 1, indicating that the produced electron neutrino at the core could transform entirely to the opposite flavor, a muon neutrino, due to the mixing in matter (in vacuum, amplitude is never maximal).

The whole propagation in the Sun is seen in Fig. 4, where significant changes compared to the low energy regime can be appreciated. Firstly, oscillation amplitude

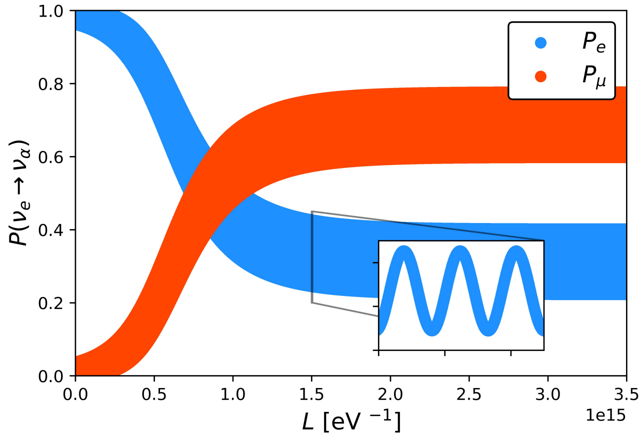

Figure 4: Probability of oscillation in function of traversed distance L throughout the propagation in the Sun.

is now much smaller than in previous cases, meaning the state is at all times close to being an eigenstate of the Hamiltonian. This eigenstate starts being a flavor eigenstate and slowly transitions to a mass eigenstate almost adiabatically, hence the use of adiabatic approximation to solve the differential equation. Furthermore, once it becomes a mass eigenstate the probability stays constant as the matter potential loses the advantage over the vacuum term, and arrives at Earth detectors as a mass eigenstate too.

B. Non-Standard Interactions (NSI)

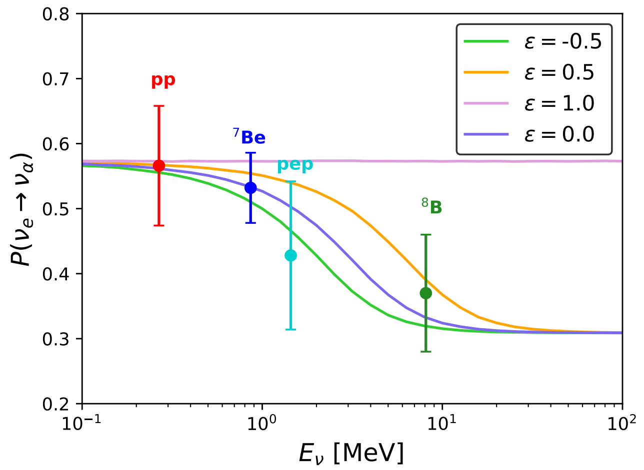

Figure 5: Survival probability of an electron neutrino in function of its energy E_ν for different values of the diagonal NSI ε', and the latest experimental points and corresponding uncertainty of the pp, pep, ^{7}Be and ^{8}B neutrinos [10].

As expected, in Fig. 5 it can be observed that by setting ε' to zero the standard case is recovered and the probability remains unaffected. When setting $\varepsilon' = 1$, matter potential is multiplied by zero and the Hamiltonian becomes the vacuum one, as shown in Eq. 6. This line overlaps with the theoretical probability value in vacuum, 0.57. Even when introducing diagonal NSI, the results at low and high energies recover the theoretical values of the adiabatic approximation (Eq. 7).

It is interesting to notice how the experimental values are all compatible with NSI, both the positive and negative value of ε, which shows that an interaction outside of the Standard Model parametrized by these ε is in agreement with the found data. However, error bars are too large to rule out any possibility, not narrowing the requirements of this interaction.

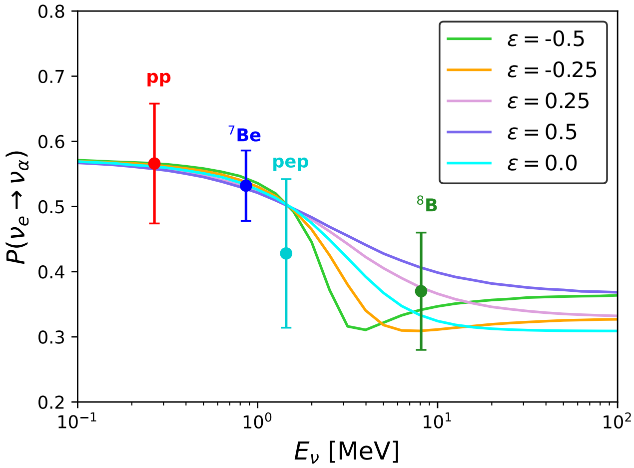

Figure 6: Survival probability of an electron neutrino in function of its energy E_ν for different values of the non-diagonal NSI ε_{nd}, and the latest experimental points and corresponding uncertainty of the pp, pep, ^{7}Be and ^{8}B neutrinos [10].

In Fig. 6, as in diagonal NSI, the chosen range of the interaction strength parameter $-0.5 \leq \varepsilon_{nd} \leq 0.5$ is entirely compatible with experimental data, with a high coincidence for the two lowest energy points, corresponding to pp and ^{7}Be neutrinos. The uncertainties in experimental values do not constrain the strength of the NSI in this studied range.

IV. CONCLUSIONS

In this work we have successfully studied neutrino oscillations in vacuum and under a matter potential, known as the MSW or matter effect over the whole relevant energy spectrum. The MSW effect influences oscillations increasing with energy and becoming completely dominant at high energies, an outcome that matches both the theoretical and experimental results and shows accurately the validity of the adiabatic approximation. Moreover, the simulation has included Non-Standard Interactions to analyze the impact of these new interactions that deviate from the Standard Model and we have concluded that for diagonal interactions, an ε parameter ranging from -0.5 to 0.5 is compatible with the latest experimental results of neutrino detection. For non-diagonal interactions (ND-NSI), the considered ε values in the same range as for the diagonal NSI all agree with neutrino detections. Nevertheless, in the high energy limit for ND-NSI the probabilities obtained deviate from the adiabatic approximation prediction albeit in the low energy limit all the curves match perfectly with experimental data of pp and ^{7}Be neutrinos.

The upcoming future experiments DUNE, JUNO and Hyper-K, covering long and medium baselines, might help narrowing the range of possible interactions and provide further information about them, in addition to having a chance at solving other open questions in this field such as CP violation and whether the mass hierarchy is normal or inverted, problems that fall beyond the scope of this project.

Acknowledgments

I would like to sincerely thank my advisor, Dr. Jordi Salvadó, who has not only made this work interesting but also fun to develop. I also thank my friends for their continued support.

[1] S. Chen and X.-J. Xu, *Solar neutrinos* (2025).
[2] J. Bahcall, M. Pinsonneault, and S. Basu, The Astrophysical Journal **555**, 990 (2001).
[3] R. Bahcall, J. N.; Davis, Science **191**, 264 (1976).
[4] L. Wolfenstein, Physical Review D **17**, 2369–2374 (1978).
[5] S. P. Mikheyev and A. Y. Smirnov, Yadernaya Fizika **42**, 1441 (1985).
[6] I. Esteban, M. C. Gonzalez-Garcia, M. Maltoni, I. Martinez-Soler, J. P. Pinheiro, and T. Schwetz, Journal of High Energy Physics (2024).
[7] M. C. Gonzalez-Garcia and Y. Nir, Reviews of Modern Physics **75**, 345–402 (2003).
[8] S. K. and Agarwalla et al., Journal of High Energy Physics **2020** (2020).
[9] O. G. Miranda and H. Nunokawa, New Journal of Physics **17**, 095002 (2015).
[10] T. B. Collaboration, Nature **562**, 505–510 (2018).

Propagació de neutrins al Sol: estudi de l'efecte MSW

Author: Marta Giral López, mgirallo10@alumnes.ub.edu
Facultat de Física, Universitat de Barcelona, Diagonal 645, 08028 Barcelona, Spain.

Advisor: Jordi Salvadó, jsalvado@ub.edu

Resum: El descobriment de les oscil·lacions de neutrins va resoldre el problema dels neutrins solars, però contradiu el Model Estàndard degut a que implica que els neutrins tenen massa, suggerint l'existència d'una nova física més enllà del Model Estàndard. En aquest treball s'estudia l'impacte de l'efecte MSW en oscil·lacions de dos neutrins via simulació numèrica, i es comparen els resultats amb l'aproximació adiabàtica (resolució analítica) i les dades experimentals més recents dels detectors de neutrins. La resolució numèrica permet incorporar interaccions no estàndard parametritzades per un escalar ε, pesades respecte del potencial de matèria. Els resultats indiquen que els valors numèrics són compatibles amb l'aproximació adiabàtica i amb les interaccions estàndard i no estàndard pel rang d'ε estudiat, no estan restringits per les dades experimentals.
Paraules clau: Neutrins solars, oscil·lacions de neutrins, efecte MSW, interaccions no estàndard.
ODSs: Educació de qualitat (ODS 4); Indústria, innovació, infraestructures (ODS 9); Reducció de les desigualtats (ODS 10).

Objectius de Desenvolupament Sostenible (ODSs o SDGs)

1. Fi de la es desigualtats		10. Reducció de les desigualtats	X
2. Fam zero		11. Ciutats i comunitats sostenibles	
3. Salut i benestar		12. Consum i producció responsables	
4. Educació de qualitat	X	13. Acció climàtica	
5. Igualtat de gènere		14. Vida submarina	
6. Aigua neta i sanejament		15. Vida terrestre	
7. Energia neta i sostenible		16. Pau, justícia i institucions sòlides	
8. Treball digne i creixement econòmic		17. Aliança pels objectius	
9. Indústria, innovació, infraestructures	X		

Appendix A: Two-neutrino evolution differential equation

The final differential equation to solve after the changes in Hamiltonian of Eq. 5 and 6 is the time-dependent Schrödinger equation in the two-neutrino framework, considering MSW effect and Non-Standard Interactions:

$$i\frac{d}{dL}\begin{pmatrix}\nu_e\\ \nu_\mu\end{pmatrix} = \left[\frac{\Delta m^2}{4E_\nu}\begin{pmatrix}-\cos 2\theta & \sin 2\theta\\ \sin 2\theta & \cos 2\theta\end{pmatrix} + \begin{pmatrix}V_e(1-\varepsilon') & \varepsilon_{nd}\\ \varepsilon_{nd} & 0\end{pmatrix}\right]\begin{pmatrix}\nu_e\\ \nu_\mu\end{pmatrix}. \tag{A1}$$

Appendix B: Vacuum numerical solution comparison

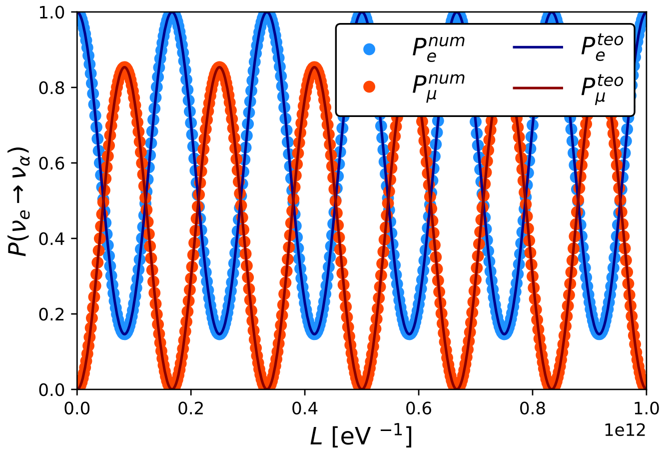

Figure 7: Probability of an electron neutrino changing its flavor (P_μ) or not (P_e) in function of traversed distance L in vacuum, for a fixed energy $E_\nu = 1$ MeV. P^{teo} are the theoretical values of the probability (Eq. 8) and P^{num} are the numerical values of the probability obtained in the simulation.

Fig. 7 shows that the numerical simulation matches perfectly the theoretical solution, with no visible deviation from it. Thus, the values from the simulation are practically exact and uncertainties are imperceptible in the all figures.